



**HAL**  
open science

## Rapid removal of fungicide thiram in aqueous medium by electro-Fenton process with Pt and BDD anodes

Moussa Mbaye, Pape Abdoulaye Diaw, Olivier Maurice Aly Mbaye, Nihal Oturan, Mame Diabou Gaye Seye, Clément Trelu, Atanasse Coly, Alphonse Tine, Jean-Jacques Aaron, Mehmet A Oturan

### ► To cite this version:

Moussa Mbaye, Pape Abdoulaye Diaw, Olivier Maurice Aly Mbaye, Nihal Oturan, Mame Diabou Gaye Seye, et al.. Rapid removal of fungicide thiram in aqueous medium by electro-Fenton process with Pt and BDD anodes. *Separation and Purification Technology*, 2022, 281, pp.119837. 10.1016/j.seppur.2021.119837 . hal-03582528

**HAL Id: hal-03582528**

**<https://hal.science/hal-03582528>**

Submitted on 16 Oct 2023

**HAL** is a multi-disciplinary open access archive for the deposit and dissemination of scientific research documents, whether they are published or not. The documents may come from teaching and research institutions in France or abroad, or from public or private research centers.

L'archive ouverte pluridisciplinaire **HAL**, est destinée au dépôt et à la diffusion de documents scientifiques de niveau recherche, publiés ou non, émanant des établissements d'enseignement et de recherche français ou étrangers, des laboratoires publics ou privés.



Distributed under a Creative Commons Attribution - NonCommercial 4.0 International License

# Rapid removal of fungicide thiram in aqueous medium by electro-Fenton process with Pt and BDD anodes

Moussa Mbaye<sup>1,2</sup>, Pape Abdoulaye Diaw<sup>1,2,3</sup>, Olivier Maurice Aly Mbaye<sup>1,2</sup>, Nihal Oturan<sup>2</sup>, Mame Diabou Gaye Seye<sup>1,2</sup>, Clément Trellu<sup>2</sup>, Atanasse Coly<sup>1</sup>, Alphonse Tine<sup>1</sup>, Jean-Jacques Aaron<sup>2</sup>, Mehmet A. Oturan<sup>2,\*</sup>

<sup>1</sup> Lab. Photochimie et d'Analyse, Université C. A. Diop, Dakar, Sénégal.

<sup>2</sup> Université Gustave Eiffel, Laboratoire Géomatériaux et Environnement EA 4508, 77454 Marne-la-Vallée, Cedex 2, France

<sup>3</sup> Lab. Matériaux, Electrochimie et Photochimie Analytique, Université A. Diop, Bambey, Sénégal

\*Corresponding author Email: Mehmet.Oturan@univ-paris-est.fr

## Abstract

The electro-Fenton (EF) process was used to assess the electrochemical degradation of the fungicide thiram and its complete removal from water using an undivided electrolytic cell equipped with Pt or BDD anode and carbon felt cathode. Hydroxyl radicals, produced homogeneously in bulk solution from electrochemically generated Fenton's reagent ( $\cdot\text{OH}$ ) and heterogeneously on the anode surface ( $\text{M}(\cdot\text{OH})$ ) from oxidation of water, reacted with thiram leading to its fast oxidation. Oxidative degradation and mineralization kinetics were monitored by chromatographic analysis (HPLC) and total organic carbon (TOC) measurements. The electrochemical degradation of thiram by hydroxyl radicals followed a pseudo-first-order reaction kinetics with an absolute rate constant  $k_{\text{abs(Thir)}}$  of  $5.54 (\pm 0.03) \times 10^9 \text{ M}^{-1} \text{ s}^{-1}$ , determined by competition kinetics method. The TOC removal rate values were found significantly higher with BDD anode than Pt anode. Thus, almost complete mineralization (92%) of thiram solution was obtained when using BDD anode.

28 These results highlight the major role of heterogeneous BDD( $\cdot\text{OH}$ ) formed in the  
29 mineralization of thiram. The contribution of homogeneous  $\cdot\text{OH}$  in mineralization of  
30 thiram was found relatively low due to its specific aliphatic structure. The efficiency of  
31 the EF process was evaluated by determining mineralization current efficiency and energy  
32 consumption per gram of TOC removed. Degradation by-products and inorganic ions,  
33 such as nitrate ( $\text{NO}_3^-$ ), nitrite ( $\text{NO}_2^-$ ), ammonium ( $\text{NH}_4^+$ ) and sulfate ( $\text{SO}_4^{2-}$ ) formed  
34 during mineralization process, were identified by GC-MS and ionic chromatography  
35 analyses and a plausible mineralization pathway was proposed.

36 ***Keywords:***

37 Electro-Fenton; Hydroxyl radical; Thiram; Mineralization; Oxidative degradation; BDD  
38 anode; Degradation pathway

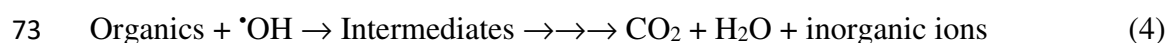
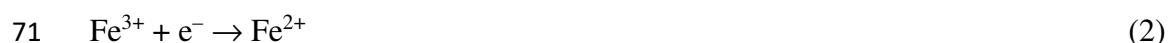
39

40 **1. Introduction**

41 Thiram is a broad spectrum contact fungicide of dithiocarbamate family widely  
42 used to control fungal diseases and to prevent crop damages. It is employed as a foliar  
43 treatment for fruits, vegetables and ornamental plants in order to control botrytis  
44 mushroom species. It is also recommended for hardy woody plants as repulsive since it  
45 is one of the most effective compound used as animal repellent to protect crops from  
46 damage by rabbits, rodents, and deer [1,2]. Moreover, it is an environmental degradation  
47 product of two other fungicides, ferbam and ziram [1]. These three pesticides are  
48 teratogens, neurotoxics, reproductive and thyroid toxins, mutagens, and skin sensitizers  
49 [3, 4]. Because of a high carcinogenic potential, thiram residues must be controlled in  
50 environmental matrices or the contaminated media should be treated.

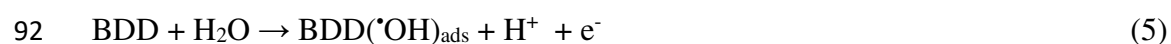
51 Advanced oxidation processes (AOPs) are currently receiving great attention [5,  
52 6, 7] for effective removal of persistent/toxic organic pollutants from water. Recently,

53 work conducted by Ganiyu et al. [8] have focused on the formation and detection of  
 54 species and reactive mechanisms. Among AOPs, Fenton and related processes (electro-  
 55 Fenton (EF), photo-Fenton, photo-EF) are widely used for removal of pesticides from  
 56 water and in treatment of industrial and pharmaceutical effluents or for wastewater reuse  
 57 [9-14]. In recent years, the EF process was also applied to the removal of polycyclic  
 58 aromatic hydrocarbons from contaminated soils [15-16]. This method is based on the  
 59 electrocatalytic generation/regeneration of Fenton's reagent ( $\text{H}_2\text{O}_2 + \text{Fe}^{2+}$ ) (Eqs. 1 and 2)  
 60 to produce *in situ* hydroxyl radicals ( $\cdot\text{OH}$ ) (Eq. 3), a strong and non-selective oxidizing  
 61 agent.  $\cdot\text{OH}$  are very active towards organic compounds and are able to destroy them until  
 62 complete mineralization (Eq. 4). The interest of the EF process results from its capacity  
 63 to *in situ* generate the reagents required for the production of  $\cdot\text{OH}$  [17,18], in contrast to  
 64 the classical Fenton process. Indeed,  $\text{H}_2\text{O}_2$  is formed via the 2-electron reduction of  
 65 oxygen (Eq. 1), while the ferrous iron ( $\text{Fe}^{2+}$ ), added in the solution in catalytic quantity,  
 66 is continuously regenerated in the medium (Eq. 2) from the 1-electron reduction of  $\text{Fe}^{3+}$   
 67 formed during the Fenton reaction (Eq. 3) [17-22]. The importance of these  
 68 electrochemical processes lies in these abilities to be combined with other processes for  
 69 rapid and more efficient treatment [23, 24].



74 The efficiency of the EF depends on several parameters, including the nature of the  
 75 electrodes, current intensity,  $\text{Fe}^{2+}$  concentration, and pH of the medium. The use of pH 3  
 76 was demonstrated as the best value for an efficient treatment [17,18]. Özcan et al. [25]

77 and Sopaj et al. [26] comparatively investigated the capacities of different cathode  
78 materials such as carbon sponge, carbon felt, graphite and stainless steel as well as the  
79 impact of current on the generation of H<sub>2</sub>O<sub>2</sub>. The use of several types of anodes (active  
80 and non-active), including Pt, Ti/RuO<sub>2</sub>-IrO<sub>2</sub>, Ti/RuO<sub>2</sub>-TiO<sub>2</sub>, dimensionally stable anode  
81 (DSA), SnO<sub>2</sub>, Ti<sub>4</sub>O<sub>7</sub>, PbO<sub>2</sub>, and boron-doped diamond (BDD), has also been investigated  
82 for application in the EF process [27-30]. BDD anode has received a great attention due  
83 to its high overpotential for O<sub>2</sub> evolution reaction, large potential window, chemical  
84 stability, high corrosion resistance, low background currents, high chemical inertness and  
85 long-term response stability [31]. The oxidation with BDD consists to a simple electron  
86 transfer processes in region of water stability ( $E < 2.3$  V vs. SHE) or in the potential  
87 region of water decomposition ( $E > 2.3$  V vs. SHE) for more complex mechanism  
88 reactions [31]. Thus allowing the formation of free hydroxyl radicals and of slightly  
89 adsorbed hydroxyl radicals (BDD(\*OH)) on its surface according to Eq. 5. These radicals  
90 were shown to be able to destroy all recalcitrant organic pollutants in a non-selective way  
91 [32-34].



93 In this study, the objective was to investigate for the first time the application of  
94 the EF process to the removal of thiram (an emerging pollutant) from water. Particularly,  
95 the study focuses on the degradation kinetics of thiram and mineralization of its aqueous  
96 solution by the EF process using a carbon felt as cathode and two different anodes (Pt and  
97 BDD). A particular attention was paid to understanding the link between the different  
98 behaviors in terms of mineralization efficiency and the chemical structure of thiram.  
99 Indeed, this molecule does not include aromatic moieties or unsaturated bonds, excluding  
100 thus addition reactions of \*OH. The degradation kinetics and intermediates formed during  
101 the oxidation of thiram were followed until formation of end-products by HPLC, GC-MS

102 and ionic chromatography. A plausible degradation pathway for the mineralization of  
103 thiram in aqueous medium was also proposed. Mineralization rate and mineralization  
104 current efficiency (MCE) were determined by monitoring the TOC decay. Finally, the  
105 energy consumption per gram of TOC removed was also evaluated in order to obtain an  
106 economic insight on the process.

107

108

## 109 **2. MATERIAL AND METHODS**

110

### 111 **2.1. Chemicals**

112 Thiram (Dimethylcarbamothioylsulfanyl *N,N*-dimethylcarbamdithioate, purity >  
113 99%) (Table SM-1), methanol, anhydrous sodium sulfate, anhydrous potassium sulfate  
114 (purity > 99%), iron chloride (FeCl<sub>3</sub>) and sodium chloride were purchased from Sigma-  
115 Aldrich and used as received. Carboxylic acids and other chemicals utilized in  
116 chromatographic analysis were supplied by Sigma-Aldrich, Fluka and Acros Organics  
117 (purity > 99%). Sulfuric acid (purity > 98%) and hexahydrated ferrous sulfate (99.5%)  
118 were obtained from Acros Organics. All solutions were prepared with ultra-pure water,  
119 obtained from a Millipore Milli-Q system (resistivity > 18 MΩ.cm at room temperature).  
120 4-hydroxybenzoic acid (HBA) (purity = 99.7%) from Prolabo was used as the  
121 competition substrate in the kinetic experiments.

122

### 123 **2.2 Instrumentation and analytical procedures**

#### 124 **2.2.1. Electrochemical measurements**

125 Electrolyses were performed in a batch reactor of 250 mL capacity. Experiments  
126 were carried out using 230 mL thiram solutions of 19.2 mg L<sup>-1</sup> (0.08 mM) concentration.

127 A triple Power Supply HM7042-5 (Germany) was used to monitor electrolyses and  
128 measure the electrical charge passed. Prior to the electrolyses, compressed air was  
129 continuously supplied to the reaction medium by bubbling at flow rate of 1.0 L min<sup>-1</sup>. The  
130 cathode was a carbon felt piece covering the internal inner wall of the cell. The anode was  
131 either a Pt cylindrical grid or a 24-cm<sup>2</sup> BDD thin film prepared by HF CVD (hot filament  
132 chemical vapor deposition technique) and deposited on conductive Nb substrate  
133 (CONDIAS, Germany) placed in the center of the electrochemical cell. Aqueous solutions  
134 (50 mM) of Na<sub>2</sub>SO<sub>4</sub> or NaCl were used as electrolytes, and the pH was adjusted to 3.0.  
135 All the experiments were conducted in triplicate and the average values (with standard  
136 deviations below 3%) were used in the figures

### 137 **2.2.2. Chromatographic analysis**

138 Electrochemical degradation of thiram was monitored by HPLC set to 224 nm,  
139 using a Merck Lachrom liquid chromatograph, equipped with a diode array detector  
140 (DAD model L-7455) and fitted with a L-7100 model pump and a reverse-phase  
141 Purospher RP-18.5 μm, 4.6 mm (internal diameter), 250 mm column placed in a L-7350  
142 model oven (Merck) at 40°C. The mobile phase was a binary mixture water-methanol  
143 35:65 v/v, at a flow rate of 0.7 mL min<sup>-1</sup> and under 170 bar pressure. Chromatograms  
144 were treated with an EZChrome Elite software. Under these operating conditions, thiram  
145 exhibited a well-defined chromatographic peak at the retention time of 4.8 min. The  
146 generated aliphatic acids were identified and quantified by ion-exclusion HPLC, using an  
147 Altech liquid chromatography equipped with a 300-mm Supelcogel H column (ϕ = 7.8)  
148 and an UV absorption detector set at 225 nm. The mobile phase was a 1% H<sub>2</sub>SO<sub>4</sub> aqueous  
149 solution at flow rate of 0.2 mL min<sup>-1</sup>.

150 By-products formed during the degradation were extracted with ethyl acetate, then  
151 identified and followed by a GC-MS instrument (Thermo Fisher Scientific, model ISQ-

152 Trace-1300), using a split/splitless injector system, and a 0.32  $\mu\text{m}$  diameter, 15 m long  
153 column, kept in vacuum with a turbo-pump at high temperature (200 - 250  $^{\circ}\text{C}$ ). The  
154 mobile phase (helium) flux was maintained constant in the range 0.6-1.5  $\mu\text{L min}^{-1}$ . A Nist  
155 library Xcalibur software was utilized to interpret the mass spectra ( $m/z$  values ranging  
156 from 50 to 650).

157 Inorganic ions were followed by an ion chromatography system (Dionex ICS-  
158 1000 model) equipped with a conductivity detector thermostated at 35 $^{\circ}\text{C}$ , an AS4A-SC  
159 ion exchange column (4 mm x 250 mm) for anion analysis, and a CSRS cation exchange  
160 column (4 mm x 250 mm) for cation analysis. Mobile phases were either a mixture of  
161 sodium bicarbonate (1.7 mM) and sodium carbonate (1.8 mM) for anion analysis or a  
162 sulfuric acid (9 mM) solution for cation analysis. Flow rates were fixed at 2 and 1 mL  
163  $\text{min}^{-1}$ , respectively.

164

### 165 **2.2.3. Total organic carbon (TOC)**

166 TOC values of initial and EF treated thiram aqueous solutions were monitored  
167 using a Shimadzu TOC-V analyzer with Pt catalyst and oxygen gas at 150 mL  $\text{min}^{-1}$ .  
168 Catalytic combustion was performed at temperature of 680  $^{\circ}\text{C}$ . Mineralization rates were  
169 calculated to evaluate the mineralization degree of thiram according to Eq. 6, where  $\text{TOC}_0$   
170 and  $\text{TOC}_t$  are the TOC values at the initial time and at time t, respectively.

$$171 \quad \%Min = \frac{\text{TOC}_0 - \text{TOC}_t}{\text{TOC}_0} \quad (6)$$

172 Based on the values of TOC removal, the mineralization current efficiency (MCE) and  
173 energy consumption ( $E_c$ ) given by Eqs. 7 and 8, respectively, permitted to estimate the  
174 effect of applied current on the mineralization efficiency and the energetic cost of the  
175 treatment.



$$176 \quad MCE (\%) = \frac{n F V_{sol} \Delta(TOC)_{exp}}{4,32.10^7 m.I.t} \times 100 \quad (7)$$

$$177 \quad E_c (kWh(g TOC)^{-1}) = \frac{U_{cell}.I.t}{V_{sol} \Delta(TOC)_{exp}} \quad (8)$$

178 where, m is the number of carbon atoms in thiram molecule, F is the Faraday constant  
 179 (96487 C mol<sup>-1</sup>), n is the number of exchanged electrons, 4.32.10<sup>7</sup> is a conversion factor  
 180 (= 3600 s h<sup>-1</sup> x 12000 mg C mol<sup>-1</sup>), U<sub>cell</sub> is the cell average voltage (V), I is the applied  
 181 current intensity (A), t is the electrolysis time (s), V<sub>sol</sub> is the solution volume (L) and  
 182 Δ(TOC)<sub>exp</sub> is the experimental TOC decay (mg L<sup>-1</sup>) at time t.

183

### 184 3. RESULTS AND DISCUSSION

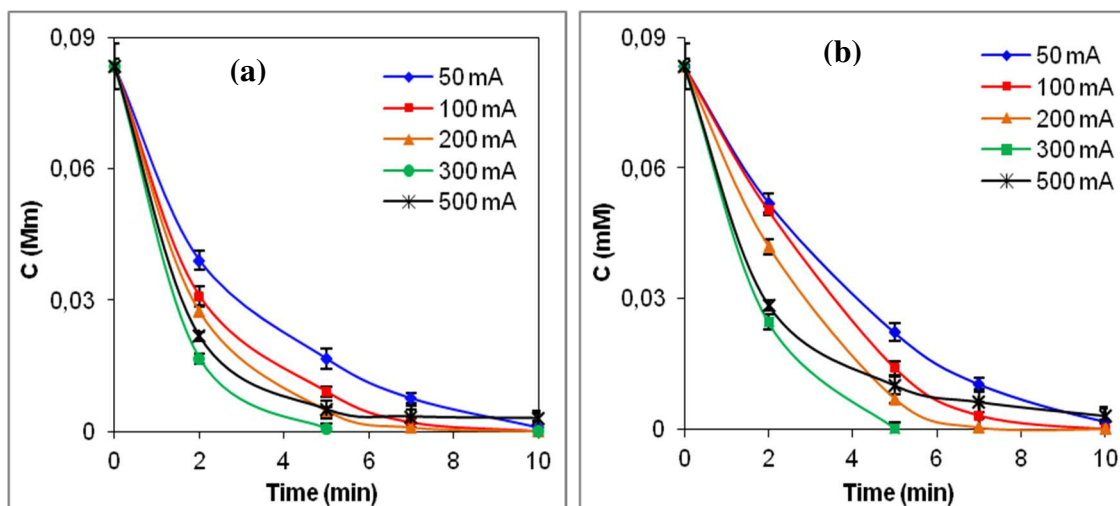
#### 185 3.1. Kinetic study of thiram degradation by the EF process

186 The effect of the current and anode type on degradation kinetics of thiram by EF process  
 187 was investigated. The decay in thiram concentration was followed by HPLC (Fig. 1) and  
 188 shows the exponential disappearance of thiram with time for Pt (a) and BDD (b) anodes,  
 189 at currents from 50 to 300 mA. The kinetic behavior of concentration decay agrees with  
 190 a pseudo-first reaction. Degradation efficiency increased with increasing current until 300  
 191 mA for which the total degradation was achieved after 5 min of electrolysis for both  
 192 anodes. However, it is worthwhile to note that above current values of 300 mA, oxidation  
 193 of thiram could be disadvantaged by parasitic reactions, mainly by the cathodic evolution  
 194 of H<sub>2</sub> and/or by further reduction of H<sub>2</sub>O<sub>2</sub> to H<sub>2</sub>O according to Eqs. 9 and 10, respectively  
 195 [33]. Besides, high currents could lead to a rapid regeneration of the catalyst Fe<sup>2+</sup>, thus  
 196 favoring the wasting reaction of \*OH in the bulk according to Eq. 11. A high current might  
 197 also favor anodic evolution of O<sub>2</sub> through the heterogeneous hydroxyl radical destruction  
 198 (Eq. 12).

209 The same trends were observed using both Pt and BDD anodes. This might be explained  
 210 by the structure of thiram, which can be easily oxidized by  $\cdot\text{OH}$  through breaking of N-C  
 211 and S-S bonds in the bulk and by  $\text{M}(\cdot\text{OH})$  on the anode surface. However, a slightly faster  
 212 degradation took place with Pt compared to BDD anode. Similar results were reported by  
 213 Sires et al. [32] during the EF degradation of antimicrobials triclosan and triclocarban.  
 214 This phenomenon can be ascribed to the strong mineralization power of BDD anode that  
 215 favors not only the oxidation of thiram but also the oxidation of its reaction intermediates  
 216 until mineralization, thus consuming oxidant species that might not be used for thiram  
 217 degradation.



212



213

214 **Fig. 1-** Effect of current on the thiram degradation kinetics during EF process with Pt (a) and BDD  
 215 (b) anodes.  $[\text{Thiram}]_0 = 0.08 \text{ mM}$ ;  $[\text{Na}_2\text{SO}_4] = 50 \text{ mM}$ ;  $[\text{Fe}^{2+}] = 0.1 \text{ mM}$ ;  $\text{pH} = 3$ ;  $V = 230 \text{ mL}$ .

216

217 **3.2 Determination of absolute rate constant for hydroxylation of thiram**

218 The degradation absolute rate constant of thiram by  $\cdot\text{OH}$  was determined in order  
219 to better understand the very fast degradation kinetics. Therefore, the absolute rate  
220 constant ( $k_{\text{abs(Thir)}}$ ) for hydroxylation of thiram was determined by using the competition  
221 of  $\cdot\text{OH}$  between thiram and the standard competitor 4-hydroxybenzoic acid (HBA); the  
222 rate constant of reaction between HBA and  $\cdot\text{OH}$  ( $k_{\text{abs, HBA}} = 2.19 \times 10^9 \text{ M}^{-1} \text{ s}^{-1}$ ) being  
223 well-known [35]. Electrolysis was carried out using a current of 50 mA on Pt anode with  
224 the same concentrations of thiram and HBA. Competition kinetics experiments were  
225 conducted at the smallest current value to avoid interference of the intermediates formed  
226 as they are accumulated in the solution due to the use of a batch reactor.

227 Simultaneous electrochemical oxidation of HBA and thiram (Eqs. 13 and 14) by  
228  $\cdot\text{OH}$  took place competitively, obeying to pseudo-first order kinetics. Because of the very  
229 short lifetimes of  $\cdot\text{OH}$ , its concentration may be considered in a quasi-stationary state.



232 The thiram degradation absolute rate constant value was thus calculated as  $k_{\text{abs(TH)}}$   
233  $= 5.54 (\pm 0.03) 10^9 \text{ M}^{-1} \text{ s}^{-1}$  from the slope of the linear plot of  $(\text{Ln} [\text{TH}]_0/[\text{TH}]_t = f$   
234  $(\text{Ln}([\text{HBA}]_0/[\text{HBA}]_t))$  (Fig. SM-1). This rate constant value was of the same order of  
235 magnitude as those found by several authors using the EF process [36-38]. For example,  
236 using the same method, Diaw et al. [33-38] found the absolute rate constant values of  
237  $4.44 \times 10^9 \text{ M}^{-1} \text{ s}^{-1}$  and  $3.1 \times 10^9 \text{ M}^{-1} \text{ s}^{-1}$  for degradation of fluometuron and monolinuron,  
238 respectively. In another example, Oturan et al. [36] used a different standard competitor,  
239 the salicylic acid (with ( $k_{\text{abs(SA)}} = 2.2 \times 10^{10} \text{ M}^{-1} \text{ s}^{-1}$ ), and found a rate constant of  $3.6 \times$   
240  $10^9 \text{ M}^{-1} \text{ s}^{-1}$  for the pentachlorophenol degradation by EF process. These values were also  
241 close to those obtained for diuron degradation by the EF process ( $k_{\text{abs(DIU)}} = 4.8 \times 10^9 \text{ M}^{-1} \text{ s}^{-1}$ ).

242  $^1 \text{ s}^{-1}$ ) and by the photo-EF process ( $k_{abs(\text{DIU})} = 4.75 \times 10^9 \text{ M}^{-1} \text{ s}^{-1}$ ) [37, 39, 40]. This high  
243 value can be assigned to the high oxidation power and non-selective character of  $\cdot\text{OH}$   
244 generated during the process and explain the rapid degradation of thiram after only 5 min  
245 of electrolysis.

246

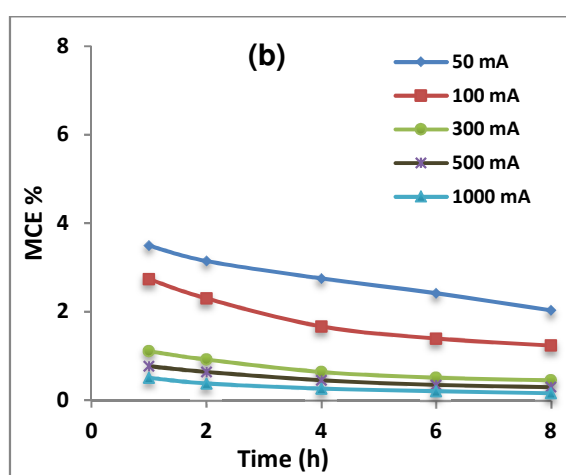
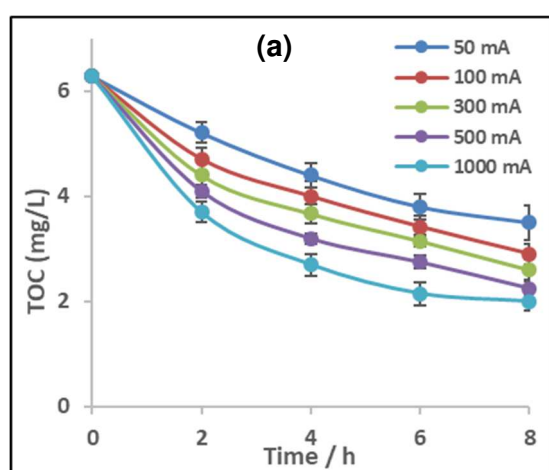
### 247 **3.3 TOC removal kinetics and mineralization efficiency**

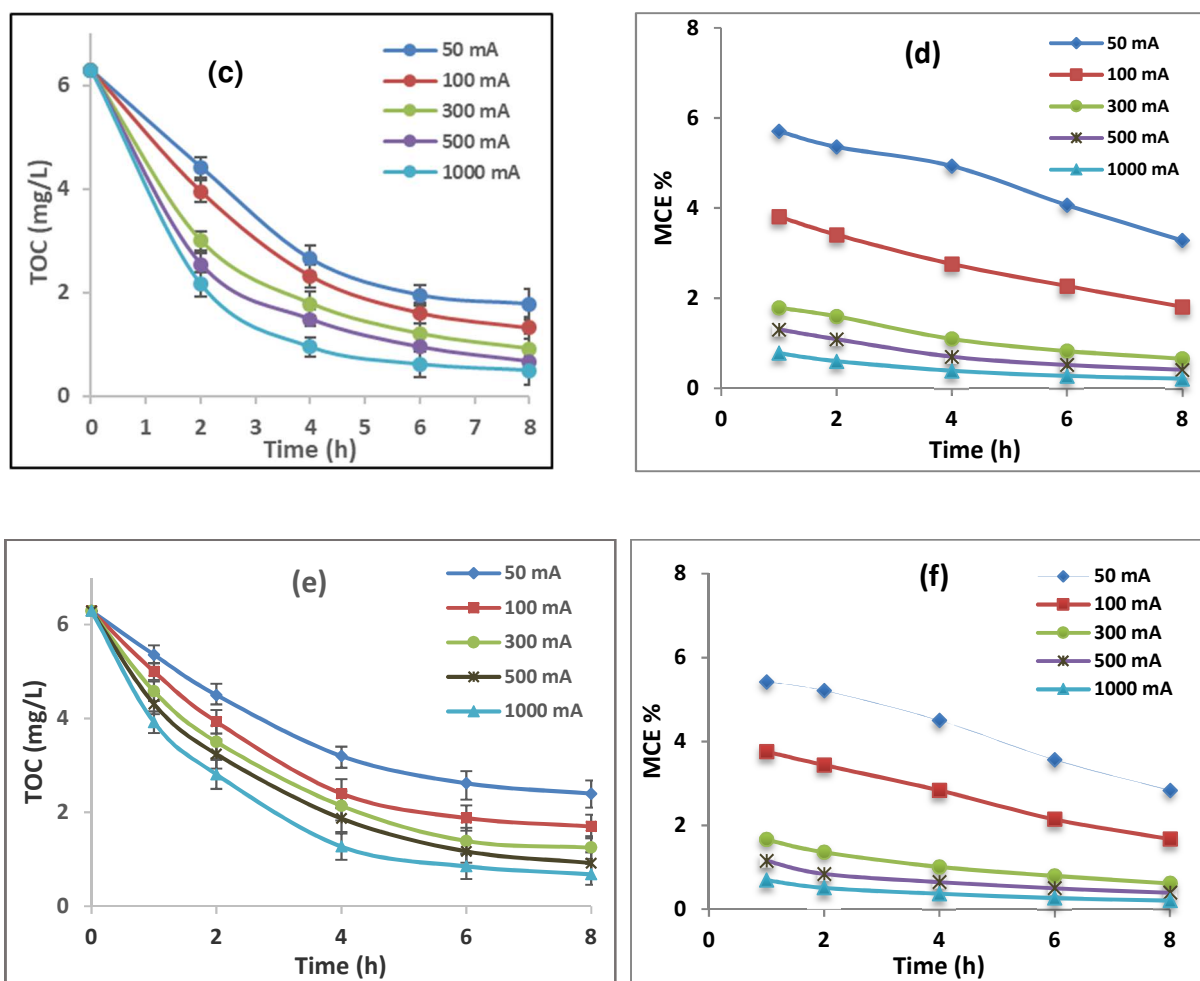
248 In order to determine the mineralization rate, TOC evolution of  $19.2 \text{ mg L}^{-1}$  ( $0.08$   
249  $\text{mM}$ ;  $\text{TOC}_0 = 5.8 \text{ mg L}^{-1}$ ) thiram solution was followed until 8 h of electrolysis by  
250 increasing the current intensity from 50 to 1000 mA (Fig. 2). As can be seen in Fig. 2a,  
251 the solution TOC decreased slowly with electrolysis time in the case of Pt anode, reaching  
252 from 44.4% to 68.2% removal rates for currents between 50 and 1000 mA, after 8 h of  
253 electrolysis. In contrast, the TOC removal efficiency is significantly higher, even in low  
254 currents, in the case of BDD anode (Fig. 2b). For example, 71.7% of solution TOC was  
255 removed at 50 mA, which is higher than the maximum value of 68.2% obtained at 1000  
256 mA with Pt anode. The TOC removal rate increased with current and attained 92% for  
257 1000 mA at 8 h. This value highlights a quasi-complete mineralization of the solution  
258 since the remaining TOC is formed of short-chain carboxylic acids which are non-toxic  
259 and biodegradable. These results evidence the major role of BDD( $\cdot\text{OH}$ ) in the  
260 mineralization of thiram solution which is also confirmed by data shown in Fig. 2c.  
261 Mineralization rate reached with anodic oxidation using BDD anode is close to the results  
262 obtained with electro-Fenton (Fig. 2b).

263 The mineralization rate of 68.2% obtained with Pt anode at 1000 mA current  
264 seems to be significantly lower compared to the literature. For instance, mineralization  
265 rates of 80% and 90% were reported by Diaw et al. [38] and Oturan et al. [41] for  
266 monolinuron and para-aminosalicylic acids, respectively, by EF treatment with Pt anode

267 at 1000 mA. The low value of rate constant found for thiram can be explained by its  
268 aliphatic structure. Indeed, the homogeneous  $\cdot\text{OH}$  are quite reactive to mineralize  
269 aromatic compounds but they have a lower mineralization power against aliphatic  
270 compounds. Moreover, Pt anode has a low overvoltage for  $\text{O}_2$ -evolution reaction and  
271 promotes oxidation of water to  $\text{O}_2$  instead of formation of large amount of  $\text{Pt}(\cdot\text{OH})$ . In  
272 addition, these  $\text{Pt}(\cdot\text{OH})$  are chemisorbed at the anode surface, thus reducing their  
273 availability for reaction with target organic compounds [42-44]. On the other hand,  
274 aliphatic compounds can be effectively mineralized when using BDD anode, particularly  
275 at high currents [43-45]. In this case, the formation of large quantities of  $\text{BDD}(\cdot\text{OH})$   
276 formed according to Eq. 5, oxidize thiram, its intermediate and end-products until  
277 mineralization in the diffusion layer of the anode surface. Therefore, TOC removal values  
278 obtained in anodic oxidation were close to those of EF processes with BDD anode. These  
279 results highlight the low contribution of homogeneous  $\cdot\text{OH}$  for the mineralization of  
280 thiram by EF with BDD anode at high current.

281





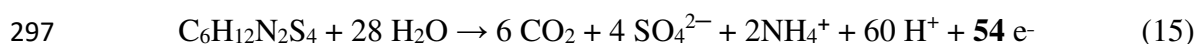
282 **Fig. 2-** Evolution of TOC and MCE during treatment of 0.08 mM thiram solution: EF with Pt (a), EF  
 283 with BDD (c) and anodic oxidation with BDD anode (e). Figures (b), (d) and (f) show the evolution  
 284 of the corresponding MCE as a function of current and electrolysis time. Experimental conditions:  
 285 pH 3;  $[Fe^{2+}] = 0.1 \text{ mM}$ ;  $[Na_2SO_4] = 50 \text{ mM}$ ;  $V = 230 \text{ mL}$ .

286

287 Besides, the slower mineralization kinetics observed on longer electrolysis time  
 288 can be explained by the enhanced limitation from mass transfer to the anode when the  
 289 bulk concentration decreases, as well as by the formation of by-products (mainly  
 290 carboxylic acids) with slower degradation kinetics [46-47]. In addition, some by-  
 291 products such as dimethyldithiocarbamate [47] could form a complex with ferric ions and

292 delay the regeneration of ferrous ions, which would subsequently decrease the  
293 mineralization kinetic.

294 To evaluate the mineralization efficiency of the EF process in thiram removal, the  
295 MCE was assessed by using the Eq. 7, taking into account the number n of electron  
296 exchanged by mole of thiram according to the mineralization reaction (Eq. 15).

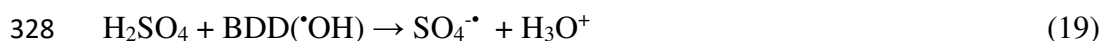
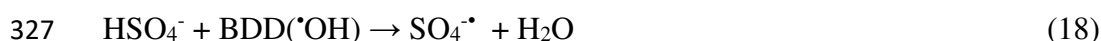
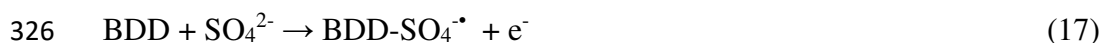


298 The evolution of MCE% was depicted in Figs. 3b, 3d and 3f for EF-Pt, EF-BDD and AO-  
299 BDD, respectively. MCE% values are relatively higher for short electrolysis times and  
300 low currents and decrease strongly at high currents of 300-1000 mA. The EF with BDD  
301 anode showed better MCE% in accordance with its high mineralization efficiency  
302 followed by anodic oxidation process while EF with Pt anode exhibited low  
303 mineralization efficiency. These results are consistent with the mineralization rates  
304 obtained with Pt and BDD anodes.

305 The energy consumption (Ec) in kWh per gTOC removed was larger with Pt anode than  
306 with BDD anode (Table 1) in agreement with TOC removal rate at the same currents and  
307 electrolysis times. Anodic oxidation with BDD anode provided Ec results close to those  
308 obtained in EF-with BDD. Overall the Ec values are low, however, it is relatively high at  
309 high currents indicating that mineralization efficiency could be affected by wasting  
310 reactions [17, 18], as shown in Eqs. (11) and (16), as well as side reactions (Eqs. (10) and  
311 (12)) and formation of Fe(III) carboxylic acid complexes [48-56]. Nonetheless, the use of  
312 renewable energies such as solar and wind can reduce energy cost [61].

313 The formation of the recalcitrant complexes could retard the mineralization in the case of  
314 Pt anode, leading to an increase of the consumed energy. According to Sirés et al. [57],  
315 these Fe(III)-carboxylato complexes might be easily destroyed by BDD ( $\cdot\text{OH}$ ), but

316 difficultly by homogeneous  $\cdot\text{OH}$  or by  $\text{Pt}(\cdot\text{OH})$ . Thus, oxidation efficiency can be  
 317 inhibited with a major consequence of increasing energy consumption, mainly in the case  
 318 of Pt anode [17-19, 58, 59]. In addition, supplementary oxidative species such as sulfate  
 319 radicals ( $\text{SO}_4^{\cdot-}$ ) can form in the medium (Eq. 17) by interaction between BDD anode and  
 320 sulfate ions [60] which from electrolyte ( $\text{Na}_2\text{SO}_4$ ) and catalyst ( $\text{FeSO}_4$ ) used.  $\text{SO}_4^{\cdot-}$  ( $E^\circ =$   
 321  $2.44 \text{ V|SHE}$ ) is slightly milder than  $\cdot\text{OH}$  but its electrophilic nature and long lifetime (30-  
 322 40 ns) offer a great opportunity for wastewater treatment. The efficiency of treatment with  
 323 BDD can be explain by the simultaneous production of  $\cdot\text{OH}$  and possible  
 324 electrogeneration of  $\text{SO}_4^{\cdot-}$  (Eqs. (18) and (19)) during electrolysis.



329  
 330 **Table 1.** Evolution of energy consumption ( $E_c$ ) in kWh per gTOC with current during the treatment  
 331 of thiram solutions by EF and anodic (AO) processes as a function of electrolysis time, under the  
 332 operating conditions of Fig. 2.

Process	Current (mA)	Electrolysis time (h)				
		1	2	4	6	8
EF-Pt	50	0.87	0.96	1.09	1.23	1.47
	100	1.21	1.44	1.97	2.35	2.67
	300	4.00	4.83	6.93	8.60	9.76
	500	7.40	8.97	12.80	17.02	19.80
	1000	13.80	18.50	27.77	36.23	46.21



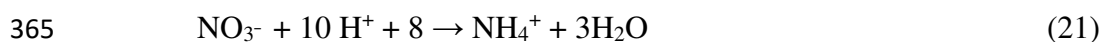
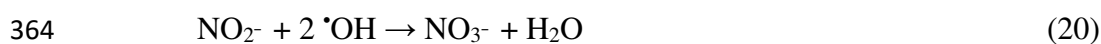
EF-BDD	50	0.59	0.62	0.65	0.86	1.09
	100	1.06	1.20	1.52	1.92	2.48
	300	3.26	3.67	5.37	7.21	9.15
	500	5.39	6.51	10.14	14.00	16.33
	1000	11.22	14.70	21.76	32.67	43.56
AO-BDD	50	0.66	0.68	0.73	0.96	1.19
	100	1.13	1.24	1.51	1.85	2.32
	300	3.45	3.54	5.04	6.85	8.72
	500	5.17	6.01	9.56	13.27	15.40
	1000	10.96	13.36	20.12	31.70	42.82

333

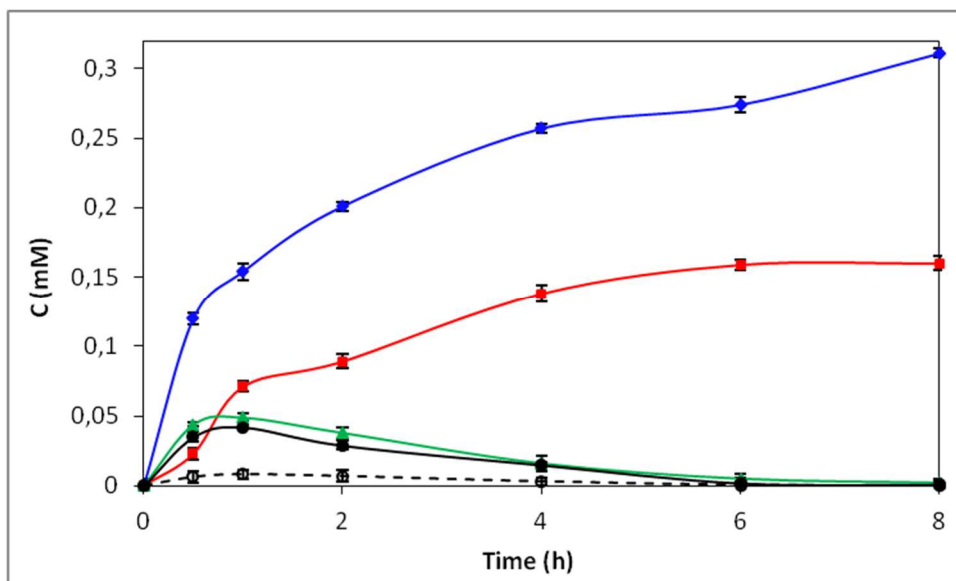
#### 334 **3.4. Formation and evolution of generated carboxylic acids and inorganic ions**

335 Treatment of organic compounds by electrochemical advanced oxidation  
336 processes generally leads to the formation of carboxylic acids as end-products before  
337 mineralization. Oxalic, acetic, malonic or oxamic (in case of N-containing compounds)  
338 are the most frequently generated short-chain carboxylic acids. However, the structure of  
339 thiram (without aromatic moiety and unsaturated bonds) does not lead to the formation  
340 of such carboxylic acids. Therefore, only the formic acid (in good agreement with the  
341 carbonic chain of thiram) was detected during mineralization experiments. Fig. 3 shows  
342 the formation and accumulation of a weak quantity of formic acid (0.008 mM after 1-h  
343 electrolysis) because of its subsequent mineralization. This result confirms the rapid  
344 transformation of thiram into CO<sub>2</sub> molecules, due mainly to the non-selective oxidation  
345 of aliphatic chains by M(<sup>•</sup>OH) at the vicinity of the BDD anode.

346 Mineralization of thiram also led to the formation of inorganic ions, including  
347 sulfate ( $\text{SO}_4^{2-}$ ), ammonium ( $\text{NH}_4^+$ ), nitrate ( $\text{NO}_3^-$ ) and nitrite ( $\text{NO}_2^-$ ) ions (Fig. 3). It is  
348 worthy to note that thiram desulfurization led to the formation of about 0.31 mM  $\text{SO}_4^{2-}$   
349 ion after 8 h of electrolysis corresponding to almost total S atom concentration of the  
350 initial solution, in agreement with the presence of four S atoms in the thiram molecule.  
351 The sum of N-containing ions reached a maximum concentration of 0.16 mM ( $[\text{NO}_2^-] +$   
352  $[\text{NO}_3^-] + \text{NH}_4^+$ ) after 1 h of electrolysis, corresponding to the total nitrogen concentration  
353 from the initial molecule (two N atoms). This result indicates that all the nitrogen was  
354 rapidly removed from thiram. After the first hour of electrolysis,  $\text{NO}_2^-$  and  $\text{NO}_3^-$   
355 concentrations decreased gradually, whereas  $\text{NH}_4^+$  concentration increased progressively  
356 and reached a maximum concentration of 0.15 mM after 6 h electrolysis (Fig. 3). This  
357 phenomenon might be explained by the reduction of  $\text{NO}_2^-$  (Eq. 20) and  $\text{NO}_3^-$  (Eq. 21) ions  
358 into  $\text{NH}_4^+$  at the carbon felt cathode [48, 49]. Similar behavior was also observed by other  
359 researchers. For example, Özcan et al. [50] and Diagne et al. [51] reported same behavior  
360 during the EF treatment of the azinphosmethyl and methyl parathion insecticides,  
361 respectively. Mousset et al. [52] and El-Ghenymy et al. [53] also found a similar evolution  
362 of N and S-containing ions during the treatment of synthetic wastewater by the EF and  
363 sulfanilic acid by the solar photo-EF processes, respectively.



366



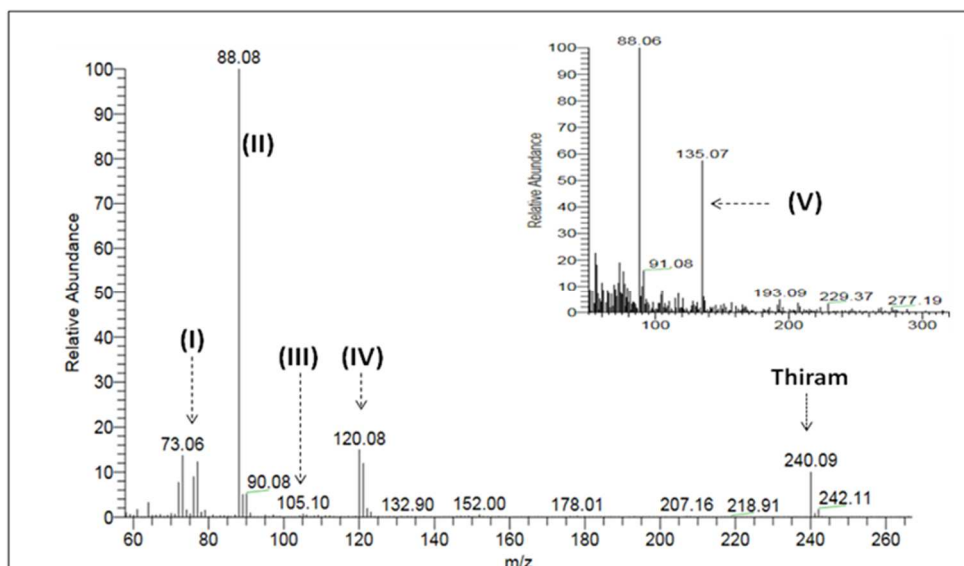
367

368 **Fig. 3-** Evolution of formic acid (- -○- -) and inorganic ions: (-◆-) SO<sub>4</sub><sup>2-</sup>; (-■-) NH<sub>4</sub><sup>+</sup>; (-△-) NO<sub>3</sub><sup>-</sup>; and  
 369 (-●-) NO<sub>2</sub><sup>-</sup>, formed during the EF treatment of 0.08 mM thiram. Experiments were conducted using  
 370 0.1 mM FeCl<sub>3</sub> (as catalyst source) and 50 mM NaCl (as electrolyte) in order to avoid the interference  
 371 with sulfate detection. Other conditions: BDD anode, I = 500 mA, pH = 3, and V = 230 mL.

372

### 373 3.5 Identification of thiram by-products and mineralization pathways

374 Several thiram by-products formed during the oxidative degradation of thiram by EF  
 375 treatment were detected by GC-MS analysis, after extraction with ethyl acetate. Among  
 376 them, five intermediates, including carbon disulfide (**I**), 1,1,2,2-tetramethylhydrazine  
 377 (**II**), N,N-dimethylthiocarbamoic acid (**III**), dimethyldithiocarbamate (**IV**) and N,N-  
 378 dimethyl S-hydroxydithiocarbamate (**V**), were identified by means of mass spectrum  
 379 characteristics (Table 2). Figure 4 shows the mass spectra of the solution containing  
 380 thiram by-products obtained by EF treatment with a BDD anode after 5 min (Fig. 4) and  
 381 10 min (insert of Fig. 4), respectively, at 50 mA.



382

383 **Fig. 4-** Mass spectra of 19.2 mg L<sup>-1</sup> (0.08 mM) thiram by-products solution obtained after 5 and 10  
 384 min (insert) electrolyzes by the EF process with BDD anode at applied current of 50 mA.

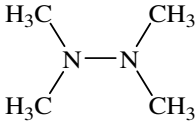
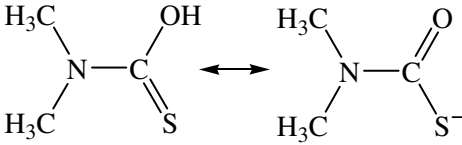
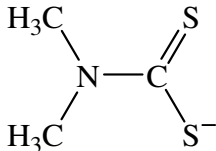
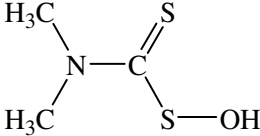
385

386 Based on the identified by-products, a plausible mineralization pathway was  
 387 proposed (Fig. 5). Oxidative degradation of thiram by <sup>•</sup>OH led to the cleavage of C-N  
 388 bonds, yielding dimethyl-amine radicals that conducts to the formation of the dimer **II**  
 389 after rearrangement (Table 2). Compound **IV** was obtained by breaking the S-S bond  
 390 under oxidative attack of <sup>•</sup>OH and then led to the formation of the carbon disulfide (**I**)  
 391 through breaking of N-C bond. The appearance of these three by-products took place in  
 392 acidic medium (pH = 3), in agreement with former results from Joris et al. [62]. Moreover,  
 393 oxidation of compound **IV** might led to the formation of compound **III** in its two  
 394 mesomeric forms, considered as an alcohol-protecting group [63]. In addition, compound  
 395 **IV** might undergo hydroxylation and yield compound **V**, which appeared after a 10-min  
 396 electrolysis. These by-products are in agreement with those already reported in literature  
 397 [47, 62, 64, 65] during degradation of thiram by other methods. For example, some studies  
 398 have reported the degradation of thiram by microbial action and by hydrolysis in acidic  
 399 soils [47]. The main thiram metabolites obtained under these conditions were  
 400 dimethyldithiocarbamate, dimethyl-amine and carbon disulfide (CS<sub>2</sub>). The by-products **I**

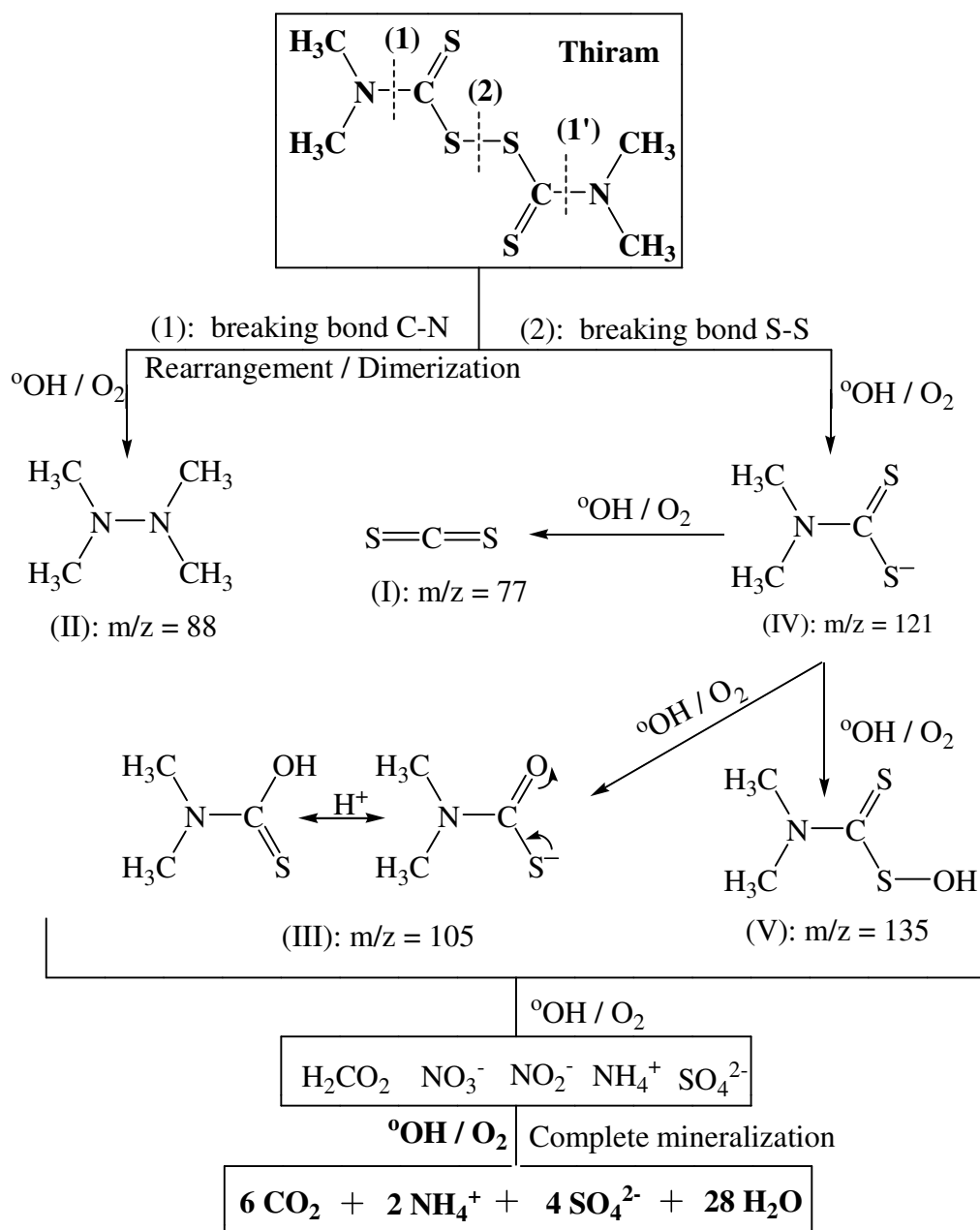
401 and **IV** were also reported by Dalvi et al. [64] during biological degradation in order to  
 402 investigate their toxicity [66].

403 On the other hand and contrary to aromatic compounds, which lead to the  
 404 formation of several carboxylic acids, only formic acid was detected as short-chain  
 405 carboxylic acid during mineralization of thiram in the EF process, because thiram  
 406 includes only -CH<sub>3</sub> group as the longest carbon-chain. The mineralization experiments  
 407 led also to the formation of different inorganic ions such as sulfate, ammonium, nitrate  
 408 and nitrite ions (Fig. 5) according to the presence of S and N atoms in the mother  
 409 pollutant.

410 **Table 2.** GC-MS identification of thiram by-products formed during the EF oxidation of a 19.2 mg  
 411 L<sup>-1</sup> (0.08 mM) initial thiram solution.

By-products	Structures	R <sub>t</sub> <sup>a</sup> (min)	m/z
carbon disulfide ( <b>I</b> )	$\text{S}=\text{C}=\text{S}$	3.11	77
1,1,2,2-tetramethylhydrazine ( <b>II</b> )		3.18	88
N,N-dimethylthiocarbamoic acid ( <b>III</b> )		16.77	105
N,N-dimethyldithiocarbamate ( <b>IV</b> )		23.59	121
N,N-dimethyl S-hydroxydithiocarbamate ( <b>V</b> )		12.19	135

412 <sup>a</sup> R<sub>t</sub> = retention time



413

414 **Fig. 5-** Plausible mineralization pathways of thiram by  $^{\circ}\text{OH}/\text{M}(^{\circ}\text{OH})$  generated during the  
 415 EF process using BDD anode at 50 mA and pH 3.

416

#### 417 4. Conclusions

418 Rapid and efficient degradation of aqueous solutions of thiram was successfully  
 419 performed using the EF process. Thiram degradation by EF process with both Pt and BDD  
 420 and carbon felt cathode was achieved within 5 min using a current of 300 mA. However,  
 421 Pt anode behaved unable to mineralize effectively thiram solution because of the lower

422 mineralization capacity of homogeneous  $\cdot\text{OH}$  to mineralize aliphatic compounds. In  
423 contrast, efficient mineralization was achieved when using BDD anode, due mainly to the  
424 production of large amounts of heterogeneous BDD( $\cdot\text{OH}$ ) at the surface of this electrode.  
425 By increasing the current applied from 300 to 1000 mA, almost complete mineralization  
426 rate ( $> 90\%$ ) was obtained in both EF and anodic oxidation with BDD anode. The attack  
427 of thiram by hydroxyl radicals obeyed to a pseudo-first order reaction kinetics, and the  
428 thiram degradation was rapid, as highlighted by the high value of the absolute rate  
429 constant ( $k_{\text{abs (TH)}} = 5,54 (\pm 0,03) 10^9 \text{ M}^{-1} \text{ s}^{-1}$ ). Based on GC-MS analysis of thiram organic  
430 by-products as well as ionic chromatography analysis of inorganic ions, a plausible thiram  
431 mineralization mechanism was proposed. Monitoring TOC during mineralization  
432 experiments also permitted to determine the mineralization current efficiency (MCE) and  
433 energy consumption ( $E_c$ ) values during thiram electrolysis. The knowledge of these  
434 parameters at laboratory scale might provide an insight of the economic cost of the EF  
435 process for the treatment of industrial effluents. The results obtained confirm that the EF  
436 method constitutes a good prospect for environmental safety in treatment of  
437 toxic/persistent organic pollutants.

#### 438 **Acknowledgements**

439 P.A. Diaw thanks the Service of Cooperation and Cultural Action (SCAC) of the French  
440 Embassy in Dakar (Senegal) for a French Cooperation Postdoc grant (Campus France  
441 **P615117E**) in support of this work.

442

## References

- [1] Sharma V.K., Aulakh J.S., Malik A.K. Thiram: degradation, applications and analytical methods. *J. Environ. Monit.* 5 (2003) 717–723.
- [2] Environmental Protection Agency. Prevention, Pesticides and Toxic Substances (7508C). EPA 738-F-04-010, USA, September 2004.
- [3] Gosselin R.E., Smith R.P, Hodge H.C. Clinical toxicology of commercial products. Fifth ed., Williams & Wilkins, Baltimore, MD, 1984.
- [4] Lee, C.C., J.Q. Russell and J.L. Minor. Oral toxicity of ferric dimethyldithiocarbamate (ferbam) and tetra methylthiuram disulfide (thiram) in rodents. *J. Toxicol. Environ. Health*, 4 (1978) 93-106.
- [5] Oturan M.A., Aaron J.J. Advanced oxidation processes in water/wastewater treatment: principles and applications. A review, *Crit. Rev. Environ. Sci. Technol.*, 44 (2014) 2577-2641.
- [6] Gogate P.R., Pandit A.B. A review of imperative technologies for wastewater treatment I: oxidation technologies at ambient conditions. *Adv. Environ. Res.*, 8 (2004) 501–551.
- [7] Martinez-Huitle C.A., Panizza M. Electrochemical oxidation of organic pollutants for wastewater treatment. *Current Opinion in Electrochemistry*, 11 (2018) 62-718.
- [8] Ganiyu S.O., Martinez-Huitle C.A., Oturan M. A. Electrochemical advanced oxidation processes for wastewater treatment: Advances in formation and detection of reactive species and mechanisms. *Current Opinion in Electrochemistry*, 27 (2021) 100678.
- [9] Hernández J.M.P., Martínez-Huitle C.A., Guzmán-Mar J.L., Ramírez A.H. Recent advances in the application of electro-Fenton and photoelectro-Fenton process for removal of synthetic dyes in wastewater treatment. *J. Environ. Eng. Manage.* 19 (5) (2009) 257-265.
- [10] Losito I., Amorisco A., Palmisano F. Electro-Fenton and photocatalytic oxidation of phenyl-urea herbicides: An insight by liquid chromatography–electrospray ionization tandem mass spectrometry. *Appl. Catal. B: Environ.*, 79 (2008) 224–236.
- [11] Oturan N., Oturan M.A. Degradation of three pesticides used in viticulture by electrogenerated Fenton's reagent. *Agron. Sustain. Dev.*, 25 (2005) 267- 270.
- [12] Brillas E., A review on the photoelectro-Fenton process as efficient electrochemical advanced oxidation for wastewater remediation. Treatment with UV light, sunlight, and coupling with conventional and other photo-assisted advanced technologies. *Chemosphere*, 250 (2020) 126198



- [13] Sina M.A., Mohsen M. Advances in Fenton and Fenton based oxidation processes for industrial effluent contaminants control-A review. *Int J Environ Sci Nat Res.* 2 (4) (2017) 555594.
- [14] Balci B., Oturan M.A., Oturan N., Sirés I. Decontamination of aqueous glyphosate, (aminomethyl) phosphonic acid, and glufosinate solutions by electro-Fenton-like process with  $Mn^{2+}$  as the catalyst. *J. Agric. Food Chem.*, 57 (2009) 4888-4894.
- [15] Trellu C., Pechaud Y., Oturan N., Mousset E., Huguenot D., van Hullebusch E.D. Esposito G., Oturan M.A. Comparative study on the removal of humic acids from drinking water by anodic oxidation and electro-Fenton processes: mineralization efficiency and modelling. *Appl. Catal. B: Environ.* 194 (2016) 32-41.
- [16] Yap C.L., Gan S, Ng H.K. Fenton based remediation of polycyclic aromatic hydrocarbons-contaminated soils. *Chemosphere*, 83 (2011) 1414–1430.
- [17] Brillas E., Sirés I., Oturan M.A. Electro-Fenton process and related electrochemical technologies based on Fenton's reaction chemistry. *Chem. Rev.*, 109 (2009) 6570–6631.
- [18] Zhou M.H., Oturan M.A., Sirés I., (Eds.), *Electro-Fenton Process: New Trends and Scale-Up* (ISBN: 978-981-10-6405-0), in: *The Handbook of Environmental Chemistry*, volume 61, 2018, Springer, ISSN: 1867-979X.
- [19] Oturan N., Oturan M.A. *Electro-Fenton Process: Background, New Developments and Applications*, in: C.A. Martinez-Huitle, M.A. Rodrigo, O. Scialdone (Eds.), *Electrochemical Water and Wastewater Treatment*, Elsevier, Oxford (UK) and Cambridge (MA-USA), (2018) 193-221.
- [20] Monteil H., Péchaud Y., Oturan N., Oturan M.A., A review on efficiency and cost effectiveness of electro- and bio-electro-Fenton processes: Application to the treatment of pharmaceutical pollutants in water. *Chem. Eng. J.*, 376 (2019) 119577.
- [21] Daneshvar N., Aber S., Vatanpour V., Rasoulifard M.H. Electro-Fenton treatment of dye solution containing Orange II: Influence of operational parameters. *J. Electroanal. Chem.*, 615 (2008) 165–174.
- [22] Feng Y., Yang L., Liu J., Logan B.E. Electrochemical technologies for wastewater treatment and resource reclamation. *Environ. Sci.: Wat. Res. Technol.*, 2 (5) (2016) 800-831.
- [23] Martinez-Huitle C.A., Rodrigo M.A., Sirés I., Scialdone O. Single and coupled electrochemical processes and reactors for the abatement of organic water pollutants: A critical review. *Chem. Rev.*, 115 (2015) 13362–13407.

- [24] Sirés I., Brillas E., Upgrading and expanding the electro-Fenton and related processes. *Curr. Opin. Electrochem.* 27 (2021) 100686.
- [25] Özcan A., Sahin Y., Oturan M.A. Removal of protham from water by using electro-Fenton technology: kinetics and mechanism, *Chemosphere*, 73 (2008) 737–744.
- [26] Sopaj F., Oturan N., Pinson J., Podvorica F.I., Oturan M.A. Effect of cathode material on electro-Fenton process efficiency for electrocatalytic mineralization of the antibiotic sulfamethazine. *Chem. Eng. J.*, 384 (2020) 123249.
- [27] Panizza M., Brillas E., Comninellis C. Application of boron-doped diamond electrodes for wastewater treatment. *J. Environ. Eng. Manag.*, 18(3) (2008).139-153.
- [28] Sopaj F., Oturan N., Pinson J., Podvorica F.I., Oturan M.A. Effect of the anode materials on the efficiency of the electro-Fenton process for the mineralization of the antibiotic sulfamethazine. *Appl. Catal. B: Environmental* 199 (2016) 331-341.
- [29] Çelebi M.S., Oturan N., Zazou H, Hamdani M, Oturan M.A. Electrochemical oxidation of carbaryl on platinum and boron-doped diamond anodes using electro-Fenton technology. *Sep. Purif. Technol.*, 156 (2015) 996-1002.
- [30] Salazar-Banda G.R., Santos G.O.S., Gonzaga I.M.D., Dória A.R., Eguiluz K.I.B. Developments in electrode materials for wastewater treatment. *Curr. Opin. Electrochem.* 26 (2021) 100663.
- [31] Iniesta J., Michaud P.A., Panizza M., Cerisola G., Aldaz A., Comninellis Ch. Electrochemical oxidation of phenol at boron-doped diamond electrode. *Electrochim. Acta*, 46 (2001) 3573–3578.
- [32] Sirés I., Oturan N., Oturan M.A., Rodríguez R.M., Garrido J.A., Brillas E. Electro-Fenton degradation of antimicrobials triclosan and triclocarban. *Electrochim. Acta*, 52 (2007) 5493–5503.
- [33] Diaw P.A., Oturan N., Gaye Seye M.D., Coly A., Tine A., Aaron J.J, Oturan M.A. Oxidative degradation and mineralization of the phenylurea herbicide fluometuron in aqueous media by the electro-Fenton process. *Sep. Purif. Technol.*, 186 (2017) 197–206.
- [34] Ganzenko O., Trellu C., Oturan N., Huguenot D., Péchaud Y., van Hullebusch E. D, & Oturan M. A. Electro-Fenton treatment of a complex pharmaceutical mixture: Mineralization efficiency and biodegradability enhancement. *Chemosphere*, (2020) 126659.
- [35] Haidar M., Dirany A., Sirés I., Oturan N., Oturan M. A. Electrochemical degradation of the antibiotic sulfachloropyridazine by hydroxyl radicals generated at a BDD anode. *Chemosphere*, 91 (2013) 1304–1309.

- [36] Oturan M.A., Oturan N., Lahitte C., Trevin S. Production of hydroxyl radicals by electrochemically assisted Fenton's reagent. Application to the mineralization of an organic micropollutant, pentachlorophenol. *J. Electroanal. Chem.*, 507 (2001) 96–102.
- [37] Oturan N., Edelahi M.C., Oturan M.A., Aaron J.J., Podvorica F.I., Kacemi K.El. Comparative study of degradation of herbicide diuron residues in water by various Fenton's reaction-based advanced oxidation processes. *Proceedings of Balwois Conference - Ohrid, Republic of Macedonia*, 2010.
- [38] Diaw P.A., Oturan N., Gaye Seye M.D., Mbaye O.M.A., Mbaye M., Coly A., Aaron J.J., Oturan M.A. Removal of the herbicide monolinuron from waters by the electro-Fenton treatment. *J. Electroanal. Chem.*, 864 (2020) 114087.
- [39] Oturan M.A., Edelahi M.C., Oturan N., Kacemi K.El., Aaron J.J. Kinetics of oxidative degradation/mineralization pathways of the phenylurea herbicides diuron, monuron and fenuron in water during application of the electro-Fenton process. *Appl. Catal. B: Environ.*, 97 (2010a) 82–89.
- [40] Oturan M.A., Oturan N., Edelahi M.C., Podvorica F.I., Kacemi K.El. Oxidative degradation of herbicide diuron in aqueous medium by Fenton's reaction based advanced oxidation processes. *Chem. Engin. J.*, 171 (2011) 127–135.
- [41] Oturan N., Aravindakumar C.T., Olvera-Vargas H., Sunil Paul M.M., Oturan M.A. Electro-Fenton oxidation of para-aminosalicylic acid: Degradation kinetics and mineralization pathway using Pt/carbon-felt and BDD/carbon-felt cells. *Environ. Sci. Pollut. Res.*, 25 (2018) 20363–20373.
- [42] Panizza M., Cerisola G. Application of diamond electrodes to electrochemical processes. *Electrochim. Acta* 51 (2005) 191–199.
- [43] Oturan N., Brillas E., Oturan M.A. Unprecedented total mineralization of atrazine and cyanuric acid by anodic oxidation and electro-Fenton with a boron-doped diamond anode. *Environ. Chem. Lett.*, 10 (2012) 165-170.
- [44] Solano A.M.S., Costa de Araújo C.K., Vieira de Melo J., Hernandez J.M.P., Da Silva D.R., Martínez-Huitle C.A. Decontamination of real textile industrial effluent by strong oxidant species electrogenerated on diamond electrode: viability and disadvantages of this electrochemical technology. *Appl. Catal. B: Environ.*, 130–131 (2013) 112–120.
- [45] Garcia-Segura S., & Brillas E. Mineralization of the recalcitrant oxalic and oxamic acids by electrochemical advanced oxidation processes using a boron-doped diamond anode. *Wat. Res.*, 45(9) (2011) 2975-2984.

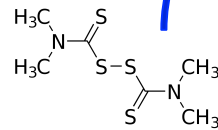
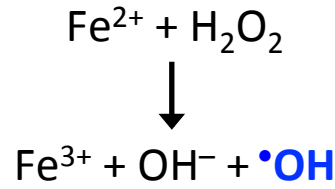
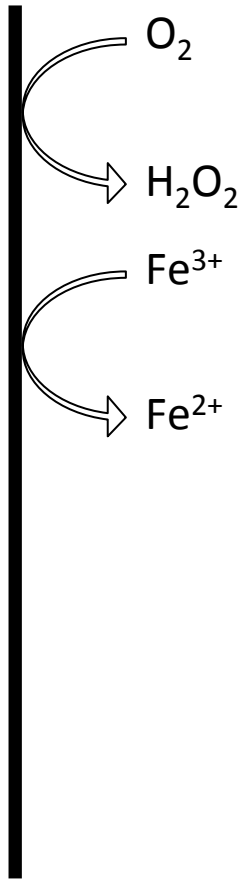
- [46] Sirés I., Arias C., Cabot P.L., Centellas F., Garrido J.A., Rodríguez R.M., Brillas E. Degradation of clofibric acid in acidic aqueous medium by electro-Fenton and photoelectro-Fenton, *Chemosphere*, 66 (2007) 1660–1669.
- [47] Howard P. H. Handbook of Environmental Fate and Exposure Data for Organic Chemicals: Pesticides, Lewis Publishers, Chelsea, MI, (1989) 4–20.
- [48] Mook W.T., Chakrabarti M. H, Aroua M.K, Khan G.M.A, Ali B.S, Islam M.S., Abu Hassan M.A. Removal of total ammonia nitrogen (TAN), nitrate and total organic carbon (TOC) from aquaculture wastewater using electrochemical technology: A review. *Desalination*, 285 (2012) 1-13.
- [49] Pérez G., Ibáñez R., Urtiaga A.M., Ortiz I. Kinetic study of the simultaneous electrochemical removal of aqueous nitrogen compounds using BDD electrodes. *Chem. Eng. J.*, 197 (2012) 475–482.
- [50] Özcan A., Sahin Y., Oturan M.A. Complete removal of the insecticide azinphosmethyl from water by the electro-Fenton method - A kinetic and mechanistic study. *Wat. Res.*, 47 (2013) 1470 - 1479.
- [51] Diagne M., Oturan N., Oturan M.A. Removal of methyl parathion from water by electrochemically generated Fenton's reagent. *Chemosphere*, 66 (5) (2007) 841-848.
- [52] Mousset, E., Pontvianne, S., Pons, M. N. Fate of inorganic nitrogen species under homogeneous Fenton combined with electro-oxidation/reduction treatments in synthetic solutions and reclaimed municipal wastewater. *Chemosphere*, 201 (2018) 6-12.
- [53] El-Ghenymy A., Segura S.G., Rodríguez R.M., Brillas E., El Begrani M.S., Abdelouahid B.A. Optimization of the electro-Fenton and solar photoelectro-Fenton treatments of sulfanilic acid solutions using a pre-pilot flow plant by response surface methodology. *J. Hazard. Mater.* 221– 222 (2012) 288– 297.
- [54] Brillas E., Boye B., Sirès I., Garrido J.A., Rodríguez R.M., Arias C., Cabot P.L., Cominellis C. Electrochemical destruction of chlorophenoxy herbicides by anodic oxidation and electro-Fenton using a boron-doped diamond electrode. *Electrochim. Acta*, 49 (2004) 4487-4496.
- [55] Olvera-Vargas H., Oturan N., Oturan M.A., Brillas E. A pre-pilot flow plant scale for the electro-Fenton and solar photoelectro-Fenton treatments of the pharmaceutical ranitidine. *Separ. Purif. Technol.*, 146 (2015) 127-137.
- [56] Rodrigo M.A., Oturan N., Oturan M.A. Electrochemically assisted remediation of pesticides in soils and water: A Review. *Chem. Rev.*, 114 (2014) 8720–8745.

- [57] Sirés I., Garrido J.A., Rodríguez R. M., Brillas E., Oturan N., Oturan M.A. Catalytic behavior of the  $\text{Fe}^{3+}/\text{Fe}^{2+}$  system in the electro-Fenton degradation of the antimicrobial chlorophene. *Appl. Catal. B: Environ.* 72 (2007) 382-394.
- [58] Oturan M.A. Outstanding performances of the BDD film anode in electro-Fenton process: Applications and comparative performance, *Curr. Opin. Solid State Mater. Sci.* 25 (2021) 100925. <https://doi.org/10.1016/j.cossms.2021.100925>
- [59] De Laat J., Le G.T., Legube B. A comparative study of the effects of chloride, sulfate and nitrate ions on the rates of decomposition of  $\text{H}_2\text{O}_2$  and organic compounds by  $\text{Fe}(\text{II})/\text{H}_2\text{O}_2$  and  $\text{Fe}(\text{III})/\text{H}_2\text{O}_2$ . *Chemosphere* 55 (2004) 715-723.
- [60] Divyapriya G., Nidheesh P.V., Electrochemically generated sulfate radicals by boron doped diamond and its environmental applications. *Curr. Opin. Solid State Mater. Sci.*, 25 (2021) 100921.
- [61] Ganiyu S.O., Martinez-Huitle C.A. The use of renewable energies driving electrochemical technologies for environmental applications. *Curr. Opin. Electrochem.* 22 (2020) 211-220.
- [62] Joris S.J., Aspila K.I., Chakrabarti C.L. Decomposition of monoalkyl dithiocarbamates. *Anal. Chem.*, 42 (6) (1970) 647-651.
- [63] Barma D.K., Bandyopadhyay A., Capdevila J.H., Falck J.R. Dimethylthiocarbamate (DMTC): An alcohol protecting group. *Org. Lett.*, 5 (25) (2003) 4755-4757.
- [64] Dalvi P.S., Kofie W.T., Mares B., Dalvi R.R., Billup L.H. Toxicologic implications of the metabolism of thiram, dimethyldithiocarbamate and carbon disulfide, mediated by hepatic cytochrome P450 isozymes in rats. *Pest. Biochem. Physiol.*, 74 (2002) 85-90.
- [65] Gupta B., Rani M., Kumar R. Degradation of thiram in water, soil and plants: a study by high performance liquid chromatography. *Biomed. Chromatogr.* 26 (2012) 69-75.
- [66] Hodgson J.R., Lee C.C. Cytotoxicity studies on dithiocarbamate fungicides. *Toxicol. Appl. Pharmacol.*, 40 (1977) 19-22.

**carbon felt  
cathode**

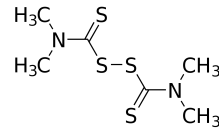
- Homogeneous vs heterogeneous  $\cdot\text{OH}$
- Reactivity of an aliphatic pollutant
  - Mineralization pathway

**Pt anode**



**fast degradation**

**BDD anode**



**fast mineralization**

$\text{M}(\cdot\text{OH})$   
 $\text{M}(\cdot\text{OH})$   
 $\text{M}(\cdot\text{OH})$   
 $\text{M}(\cdot\text{OH})$

